Eur. Phys. J. B **26**, 323–328 (2002)
DOI: 10.1140/epjb/e20020096

THE EUROPEAN
PHYSICAL JOURNAL B
EDP Sciences

Probing electron-phonon coupling in high-T_c superconductors by site-selective isotope substitution

E.Ya. Sherman[a] and C. Ambrosch-Draxl

Institute for Theoretical Physics, Karl-Franzens-University-Graz, 8010 Graz, Austria

Received 9 August 2001 and Received in final form 11 January 2002

Abstract. We consider changes in the electron-phonon coupling in high-T_c cuprates caused by site-selective oxygen isotope substitution. Contrary to the total substitution, the site-selective replacement influences the coupling constant for each phonon mode due to the induced changes in the phonon eigenvectors. The relative changes for some modes can be larger than 100%. The measured properties sensitive to these changes are discussed.

PACS. 63.20.Kr Phonon-electron and phonon-phonon interactions – 74.25.Kc Phonons

1 Introduction

Electron-phonon coupling plays an important role in normal metals and superconductors. In the normal state it renormalizes the effective mass of the carriers and leads to momentum and energy relaxation of quasiparticles being the main mechanism of the electrical resistivity in clean samples. The phonon-mediated interaction between carriers leads to the formation of Cooper pairs, *i.e.* superconductivity in conventional low-temperature superconductors [1]. In these superconductors, the isotope effect on the transition temperature leads to an approximate relationship between T_c and the atomic mass M as $T_c \sim M^{-1/2}$. The isotope effect confirms the driving role of phonons in conventional superconductivity since it shows that T_c follows the characteristic phonon frequency $\Omega \sim \sqrt{\kappa/M}$, where κ is the lattice force constant.

The discovery of the high-temperature superconducting cuprates (HTSC) resulted in an interest in the role of phonons, both in their normal state properties and the formation of the high transition temperature, which was originally assumed as arising from strong electron-phonon coupling. Many different scenarios, mostly based on magnetic fluctuation mechanisms of superconductivity have been developed over the years [2]. Early first-principles calculations of the electron-phonon coupling demonstrated that it cannot solely lead to T_c close to 100 K [3]. More recent studies have shown that electron-phonon coupling in the CuO_2 layers can support, but not cause, d-wave gap superconductivity [4–6]. Nevertheless, the effects of electron-phonon coupling are clearly seen in the normal, and the superconducting, properties of the high-T_c cuprates. It was recently proposed that coupling of electrons to the in-plane vibration of the CuO_2 plane oxygen ions can be responsible for the structure of the normal state ARPES spectra [7].

The well investigated isotope effect on T_c with ^{18}O replacing ^{16}O does not reveal the importance of phonons for the pairing. The dependence of T_c on the oxygen ion mass is doping-dependent and very weak at doping levels close to the optimum level [8]. This weakness was attributed to the fact that the energy region of the electron-electron attraction is the distance between the Van Hove singularity in the electronic spectrum at the $(0,\pi)$ point [9] and the Fermi level [10] rather than the maximal phonon frequency, which in this case becomes irrelevant for T_c. As a result the isotope effect vanishes. This effect can occur only for weak electron-phonon coupling since in the case of strong coupling the isotope effect is not sensitive to the presence of the Van Hove singularity [11]. Theoretical studies [10,11] consider the total substitution, where all oxygen ions are replaced by the other oxygen isotope. However, it is possible to produce site-selective substituted crystals with certain atomic sites filled with ^{18}O [12–17]. This substitution has two impacts on phonons: (i) it shifts the frequencies down, similar to the total substitution, (ii) it leads to changes in the eigenvectors, unlike the total substitution. The non-trivial influence of the second effect on the electron-phonon coupling will be investigated in this paper and the experimental implications will be discussed.

2 Model

As a prototype we consider the parameters of $YBa_2Cu_3O_7$, where the effect of the site-selective substitution is, theoretically, clearly seen. The shift of T_c due to the site-selective substitution in this compound has been investigated experimentally [13]. We assume that the unit cell has D_{4h} symmetry with the in-plane lattice constant $a \equiv 1$.

---

[a] On leave from the Moscow Institute of Physics and Technology, 141700, Dolgoprudny, Russia.
e-mail: `eugene.sherman@kfunigraz.ac.at`

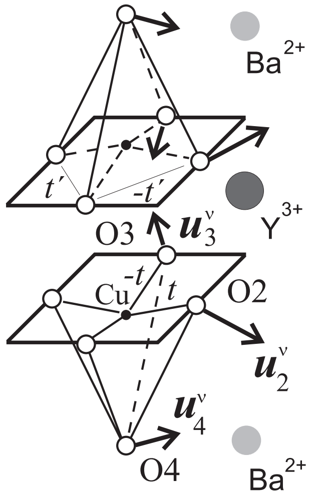

Fig. 1. Part of the unit cell considered in the model. The hopping matrix elements and the atomic displacements are defined in the text, $t\,(\mathbf{R},\mathbf{R}|1,2) = t$, $t\,(\mathbf{R},\mathbf{R}|1,3) = -t$, $t\,(\mathbf{R},\mathbf{R}|2,3) = t'$, and $t\,(\mathbf{R},\mathbf{R}'|2,3) = -t'$ if $\mathbf{R} \neq \mathbf{R}'$.

The relevant part of the unit cell is shown in Figure 1. The index ($\mathbf{R}$,r) represents the ions, where $\mathbf{R} = (R_1, R_2)$ with integer R_1 and R_2 being the position of the unit cell, and $r = 1, ..., 4$ corresponds to the Cu, O2, O3, and O4 site, respectively. Only the movement of the oxygen ions will be taken into account. For the reason which will be considered below, in the discussion of the electron-phonon coupling, we concentrate on even modes with respect to the reflection in the Y^{3+} plane. This simplification allows the consideration of only the part of the unit cell located below the Y^{3+} plane. This part has C_{4v} symmetry. For the phonon momentum $\mathbf{q} = (q_x, q_y)$ the frequencies $\Omega_\nu(\mathbf{q})$ and eigenvectors $\mathbf{U}_\nu(\mathbf{q})$ are determined by:

$$\begin{aligned} \hat{D}\,(\mathbf{q})\,\mathbf{U}_\nu(\mathbf{q}) &= \Omega_\nu^2\,(\mathbf{q})\,\mathbf{U}_\nu(\mathbf{q}), \\ \mathbf{U}_\nu^T(\mathbf{q}) &= \left[\mathbf{u}_4^\nu(\mathbf{q}), \mathbf{u}_2^\nu(\mathbf{q}), \mathbf{u}_3^\nu(\mathbf{q})\right], \end{aligned} \tag{1}$$

where $\hat{D}\,(\mathbf{q})$ is the (9×9) dynamical matrix for the oxygen atoms before the substitution, and $\mathbf{u}_4^\nu(\mathbf{q})$, $\mathbf{u}_2^\nu(\mathbf{q})$, and $\mathbf{u}_3^\nu(\mathbf{q})$ are the displacements as shown in Figure 1. The force constants in $\hat{D}\,(\mathbf{q})$ are taken to fit the frequencies and the eigenvectors of the Γ-point ($q = 0$) Raman active phonons obtained with first-principles calculations [18], which are in very good agreement with the experiment. In this point one obtains within the C_{4v} group, two A-symmetry modes (z-polarized vibrations of the apical and plane oxygen ions), one B-mode (the out-of-phase vibration along the z-axis of the plane oxygens) and three doubly degenerated E-modes, corresponding to the movement of the ions in the xy-plane. In accordance with the Raman experiments, the frequencies of the z-polarized vibrations are 500 cm^{-1} (A), 435 cm^{-1} (A), and 340 cm^{-1} (B). In the 500 cm^{-1} mode the main contribution to the eigenvector comes from the apical oxygen, while for the 435 cm^{-1} mode it is the plane oxygen ions. For this reason we will refer to these modes and those originating from them after the isotope substitution as "O4" and "O2+O3" modes. For the E-modes we take the average of the frequencies of the experimentally observed B$_{2g}$ and B$_{3g}$ modes which are given by: 550 cm^{-1} ($\mathbf{u}_{\mathrm{O2}}^\nu \parallel x$, $\mathbf{u}_{\mathrm{O3}}^\nu \parallel y$), 370 cm^{-1} ($\mathbf{u}_{\mathrm{O2}}^\nu \parallel y$, $\mathbf{u}_{\mathrm{O3}}^\nu \parallel x$), and 250 cm^{-1} for the xy-plane vibration of the apical oxygen. Some of these modes are close in frequency, and, therefore, their eigenvectors are interrelated. The z-axis displacements are coupled to each other in the Γ-point while their coupling to the in-plane displacements arises only at finite q.

Under the site-selective substitution the dynamical matrix is transformed as $\tilde{\hat{D}}(\mathbf{q}) = \hat{I}_{\mathrm{sub}}\hat{D}(\mathbf{q})\hat{I}_{\mathrm{sub}}$, with the matrices $\hat{I}_{\mathrm{sub}}$:

$$\hat{I}_{\mathrm{ap}} = \begin{bmatrix} \eta\hat{\mathrm{I}} & \hat{0} & \hat{0} \\ \hat{0} & \hat{\mathrm{I}} & \hat{0} \\ \hat{0} & \hat{0} & \hat{\mathrm{I}} \end{bmatrix}, \qquad \hat{I}_{\mathrm{pl}} = \begin{bmatrix} \hat{\mathrm{I}} & \hat{0} & \hat{0} \\ \hat{0} & \eta\hat{\mathrm{I}} & \hat{0} \\ \hat{0} & \hat{0} & \eta\hat{\mathrm{I}} \end{bmatrix}, \tag{2}$$

for the apical and plane substitution, respectively, where

$$\hat{\mathrm{I}} = \begin{bmatrix} 1 & 0 & 0 \\ 0 & 1 & 0 \\ 0 & 0 & 1 \end{bmatrix}, \qquad \hat{0} = \begin{bmatrix} 0 & 0 & 0 \\ 0 & 0 & 0 \\ 0 & 0 & 0 \end{bmatrix},$$

and $\eta = \sqrt{M(^{16}\mathrm{O})/M(^{18}\mathrm{O})} = \sqrt{8/9}$. The transformation $\hat{D}(\mathbf{q}) \to \tilde{\hat{D}}(\mathbf{q})$ leads to changes in the phonon frequencies and eigenvectors.

To obtain the electron-phonon coupling, the electronic properties of the CuO$_2$ layers are described by a tight-binding model including Cu($d_{x^2-y^2}$), O2(p_x), and O3(p_y) orbitals with the hopping t between Cu and O2 (O3), between the nearest-neighbor oxygens t', and a difference in the site energies of the Cu and O orbitals:

$$\begin{aligned} \hat{H}_{\mathrm{el}} = \varepsilon \sum_{\mathbf{R}} \hat{c}^+_{(\mathbf{R},1)}\hat{c}_{(\mathbf{R},1)} \\ + \sum_{\mathbf{R},\mathbf{R}'} \sum_{r'=2,3} \left[t\,(\mathbf{R},\mathbf{R}'|r,r')\,\hat{c}^+_{(\mathbf{R},1)}\hat{c}_{(\mathbf{R}',r')} + \mathrm{h.c}\right] \\ + \sum_{\mathbf{R},\mathbf{R}'} \sum_{r,r'=2,3} t'\,(\mathbf{R},\mathbf{R}'|r,r')\,\hat{c}^+_{(\mathbf{R},r)}\hat{c}_{(\mathbf{R}',r')}. \end{aligned} \tag{3}$$

In $\hat{H}_{\mathrm{el}}$ only the nearest-neighbor hopping for each type of the orbitals is taken into account, and the signs of the matrix elements are chosen as in Figure 1. The Bloch function of an electron with momentum $\mathbf{k}$, $\psi_{\mathbf{k}}$, has three components, corresponding to the Cu, O2, and O3 orbitals. The chosen parameters $t = 1.6$ eV, $t' = 0.35t$, and $\varepsilon = 1$ eV were used in reference [19] and are partially taken from the work of Andersen *et al.* [20]. In agreement with the experimental data of reference [21], the Fermi level is assumed to lie at 20 meV above the Van Hove singularity. We mention that the results obtained in the next section are not strongly sensitive to the parameters of the electronic subsystem.

The Hamiltonian of electron-phonon coupling for the CuO$_2$ layers will be described in terms of the Holstein model and also the dimpling-induced interaction. The Holstein model assumes changes in the one-site energies due to the ion displacements. The corresponding Hamiltonian $\hat{H}_\mathrm{e-p}^{(\mathrm{site})} = \hat{H}_\mathrm{e-p}^{(\mathrm{pl})} + \hat{H}_\mathrm{e-p}^{(\mathrm{ap})}$ is the sum of two terms:

$$\begin{aligned} \hat{H}_\mathrm{e-p}^{(\mathrm{pl})} &= C_p \sum_{\mathbf{R}} \sum_{r=2,3} \hat{c}^{+}_{(\mathbf{R},r)} \hat{c}_{(\mathbf{R},r)} \hat{z}_{(\mathbf{R},r)}, \\ \hat{H}_\mathrm{e-p}^{(\mathrm{ap})} &= C_a \sum_{\mathbf{R},\mathbf{R}'} \sum_{r=2,3} \hat{c}^{+}_{(\mathbf{R},r)} \hat{c}_{(\mathbf{R},r)} \left(\hat{z}_{(\mathbf{R}',r)} - \hat{z}_{(\mathbf{R},4)} \right), \end{aligned} \tag{4}$$

where $\hat{z}_{(\mathbf{R},r)}$ is the z-component of the ion displacement expressed in terms of phonon creation and annihilation operators. The summation in the second line of equation (4) runs over the nearest-neighbor pairs of O4 and O2, O3 ions. C_p corresponds to the change in the O2 (O3) site energy due to the displacement of the plane oxygen ions in the crystal field formed due the charge difference of the Y^{3+} and Ba^{2+} ions [22,23], while C_a is due to the interaction between the apical and the plane oxygen ions. The $\hat{H}_\mathrm{e-p}^{(\mathrm{ap})}$ contribution can arise due to direct Coulomb interaction between the apical and plane oxygen ions or due to bandstructure effects as considered by Pavarini*et al.* [24]. The other model is the interaction induced by the dimpling of the $\mathrm{CuO_2}$ layers, which allows a modulation of the hopping matrix elements $t\left(\mathbf{R},\mathbf{R}'|r,r'\right)$ by the z-axis displacements of O2 and O3 ions. The corresponding Hamiltonian has the form:

$$\hat{H}_\mathrm{e-p}^{(\mathrm{dim})} = \sum_{\mathbf{R},\mathbf{R}'} \sum_{r=2,3} C_t\left(\mathbf{R},\mathbf{R}'|r\right) \hat{c}^{+}_{(\mathbf{R}'|1)} \hat{c}_{(\mathbf{R}|r)} \hat{z}_{(\mathbf{R}|r)} + \mathrm{h.c.}, \tag{5}$$

where $C_t\left(\mathbf{R},\mathbf{R}'|r\right)$ describes the dependence of the hopping on the displacement of the plane oxygen ions. Both, $\hat{H}_\mathrm{e-p}^{(\mathrm{pl})}$ and $\hat{H}_\mathrm{e-p}^{(\mathrm{dim})}$ being proportional to the z-axis displacements of ions, arise due to the asymmetry of the cuprate layers and their environment and, therefore, should be absent if the $\mathrm{CuO_2}$ layer is flat. Since the carriers can hop between the $\mathrm{CuO_2}$ layers within the bilayer [4], shown in Figure 1, one can conclude that the phonons, which are odd with respect to the reflection in the Y^{3+} plane, can only weakly interact with the carriers, since the contributions of different layers compensate each other in these vibrations. This fact justifies the approximation of considering only the even modes.

3 Results and discussion

3.1 Self-energy effects for Raman active phonons

For further consideratios, the Hamiltonian of the electron-phonon coupling is rewritten in the momentum representation:

$$\hat{H}_\mathrm{e-p} = \sum_{\nu,\mathbf{k},\mathbf{k}'} g_\nu\left(\mathbf{k},\mathbf{k}'\right) \left[\hat{b}_{\nu,\mathbf{k}'-\mathbf{k}} + \hat{b}^{+}_{\nu,\mathbf{k}-\mathbf{k}'} \right] \hat{c}^{+}_{\mathbf{k}'} \hat{c}_{\mathbf{k}}, \tag{6}$$

where $g_\nu\left(\mathbf{k},\mathbf{k}'\right)$ is the matrix element determined by the interaction Hamiltonian, $\hat{b}_{\nu,\mathbf{k}-\mathbf{k}'}$ and $\hat{c}_{\mathbf{k}}$ are the phonon and electron annihilation operators, respectively, and $\mathbf{k}$ and $\mathbf{k}'$ are the momenta near the Fermi surface.

As the first possible experimental manifestation of the difference between the total and the site-selective substitution we consider the coupling of electrons to zero-momentum phonons. The corresponding matrix element defined as $g_\nu\left(\mathbf{k}\right) \equiv g_\nu\left(\mathbf{k},\mathbf{k}\right)$ manifests itself in the phonon self-energy effects as measured by Raman spectroscopy. The electron-phonon coupling contributes to the phonon linewidth (damping) γ_ν and leads to a renormalization of the phonon frequency Ω_ν. Linewidth and frequency are changed due to coupling of phonons to the Cooper pairs when the crystal becomes superconducting. The other effect directly related to $g_\nu\left(\mathbf{k}\right)$ is the phonon Raman intensity gain below T_c observed in different high-T_c cuprates [25,26]. The phonon self-energy effects scale as $\left|g_\nu^2\right|$, while for the intensity gain the dependence on $g_\nu\left(\mathbf{k}\right)$ is more complicated [27]. Figure 2 presents $\left|g_\nu\left(\mathbf{k}\right)\right|$ for different types of substitutions and mechanisms of electron-phonon coupling. The changes in $\left|g_\nu\left(\mathbf{k}\right)\right|$ can be either positive or negative, depending on the substituted site. By comparing two different types of substitution one can conclude that the phonon broadening and the intensity gain in the superconducting state can be changed by the site-selective isotope substitution. In the case of full substitution, $g_\nu\left(\mathbf{k}\right)$, which is proportional to the ion displacement, scales as $1/\sqrt{M\Omega}$ and decreases as $\eta^{1/2}$.

The $q=0$ phonons are probed by Raman spectroscopy. However, an analysis of the electron-phonon coupling relevant for the Raman intensity in the normal state shows that it is not always directly related to the matrix element $g_\nu\left(\mathbf{k}\right)$. For example, the Raman intensity of the plane oxygen 435 cm^{-1} mode in the case when the incident and the scattered light are polarized along the z-axis arises from the contribution of the displacement of the apical oxygen to the eigenvector of the mode. It was found by the first-principles calculations that in $\mathrm{YBa_2Cu_3O_7}$ the phonon eigenvectors at $q=0$ are strongly influenced by the site-selective substitution due to the coupling (the matrix elements D_{36} and D_{39}) of the apical and the plane oxygen displacements [18]. For this reason the site-selective replacement has a strong effect on the phonon Raman intensities [18,28]. When the apical oxygen is substituted, the difference in frequency between the apical and the plane modes becomes small. For this reason the contribution of the apical oxygen to the eigenvector of the plane mode increases leading to a strong increase in the Raman intensity. Substitution of the plane oxygen ions considerably decreases the intensity of the mode. In the case of electron-phonon coupling the changes brought by the site-selective substitution are a consequence of the same physical effect, what can be seen for the apical oxygen mode, which we take as an example. When we take into account only displacements of the plane oxygen ions $\hat{z}_{(\mathbf{R},2)}$ and $\hat{z}_{(\mathbf{R},3)}$ as in $\hat{H}_\mathrm{e-p}^{(\mathrm{pl})}$ and $\hat{H}_\mathrm{e-p}^{(\mathrm{dim})}$, the coupling of the apical phonon mode to the states in the $\mathrm{CuO_2}$ layers increases considerably with the apical substitution and decreases with the plane substitution. At the same time, the coupling of the plane modes to the electronic states in

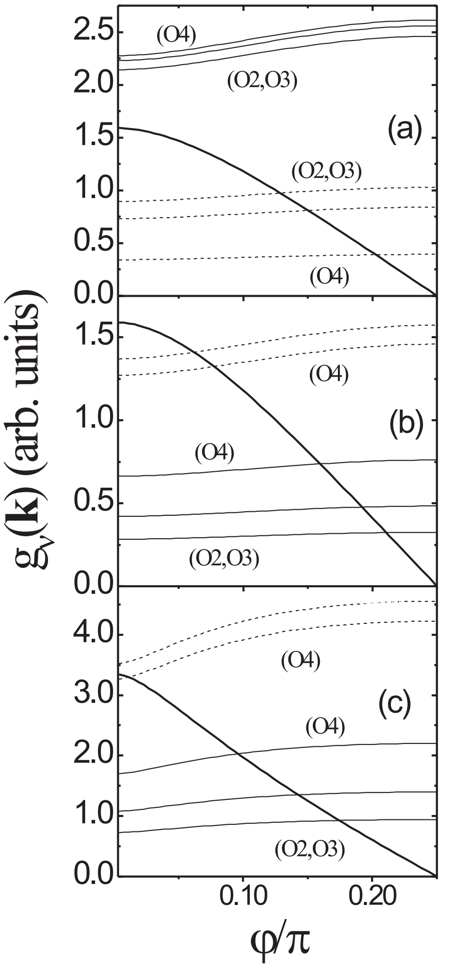

Fig. 2. The matrix elements $|g_\nu(\mathbf{k})|$ for three z-axis polarized Raman active modes. (a) $\hat{H}^{(\mathrm{ap})}_{\mathrm{e-p}}$ coupling, (b) $\hat{H}^{(\mathrm{pl})}_{\mathrm{e-p}}$ coupling, and (c) $\hat{H}^{(\mathrm{dim})}_{\mathrm{e-p}}$ coupling. Only the substituions which cause considerable changes are shown. Thin dashed and solid lines correspond to the "O4" and "O2+O3" modes, respectively. The bold line presents the "O2-O3" (B) mode. The type of the substitution is indicated near the lines. Lines without indication correspond to non-substituted crystals. The apical substitution decreases the $|g_B(\mathbf{k})|$ in the factor of $\eta^{1/2}$ (not shown in the figure). φ is the angle between the x-axis and the Fermi momentum counted from the (π,π) point, as it is shown in Figure 3.

the layers described by $\hat{H}^{(\mathrm{pl})}_{\mathrm{e-p}}$ and $\hat{H}^{(\mathrm{dim})}_{\mathrm{e-p}}$ is not strongly changed, since the displacements of the plane oxygens always give the main contribution to the eigenvector of the "O2+O3" mode. We note that the plane substitution has a very minor effect on $g_\nu(\mathbf{k})$ for this mode (not shown in Fig. 2) since the effect of the mass enhancement is compensated by the increase of the contribution of the plane oxygen displacements in the eigenvector. In addition, we mention that despite the quite different $\mathbf{k}$-dependences of $g_\nu(\mathbf{k})$ originating from $\hat{H}^{(\mathrm{dim})}_{\mathrm{e-p}}$ and $\hat{H}^{(\mathrm{pl})}_{\mathrm{e-p}}$, the relative changes introduced by the site-selective substitution are fully equivalent since in both interactions the same ionic displacements are involved.

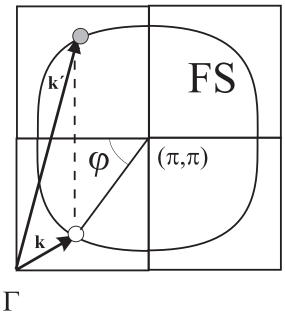

Fig. 3. The Fermi surface (a schematic plot), the momenta, and the matrix elements of the transitions forming the electron-phonon coupling in equation (7). The dashed line corresponds to the phonon, while the light and the grey circles correspond to the matrix elements $g_\nu(\mathbf{k},\mathbf{k}')$ and $g^*_\nu(\mathbf{k},\mathbf{k}')$, respectively.

3.2 Constant of electron-phonon coupling

The other possibility is the influence of the site-selective substitution on the spectrum of electrons and, in turn, the critical temperature. This effect can be described by the Eliashberg function defined as [1,29,30]:

$$\alpha^2(\omega)F(\omega) = N_F^{-1}\int\frac{\mathrm{d}l_{\mathbf{k}}}{v_{\mathrm{F}}(\mathbf{k})}\int\frac{\mathrm{d}l_{\mathbf{k}'}}{v_{\mathrm{F}}(\mathbf{k}')} \times\sum_\nu\left|g^2_\nu(\mathbf{k},\mathbf{k}')\right|\delta\left[\omega-\Omega_\nu(\mathbf{k}-\mathbf{k}')\right], \quad (7)$$

where $v_F(\mathbf{k})$ is the Fermi velocity, and N_F is the density of states at the Fermi level. The Fermi momenta $\mathbf{k}$ and $\mathbf{k}'$ are shown in Figure 3. Since we consider the cuprates, where the electron spectrum is essentially two-dimensional, the integration in equation (7) is performed over the length element of the two-dimensional Fermi line $\mathrm{d}l_{\mathbf{k}}$. For the given electron-phonon coupling one can introduce the coupling constant in the symmetry channel L as

$$\lambda_L = N_L^{-1}(0)\int\frac{\mathrm{d}l_{\mathbf{k}}}{v_F(\mathbf{k})}\sum_\nu\lambda_{L,\nu}(\mathbf{k}),$$

$$\lambda_{L,\nu}(\mathbf{k}) = \int\frac{\mathrm{d}l_{\mathbf{k}'}}{v_F(\mathbf{k}')}\phi_L(\mathbf{k})\frac{\left|g^2_\nu(\mathbf{k},\mathbf{k}')\right|}{\Omega_\nu(\mathbf{k}-\mathbf{k}')}\phi_L(\mathbf{k}'), \quad (8)$$

where $\phi_L(\mathbf{k})$ are the Fermi-line harmonics normalized as $\langle\phi_L(\mathbf{k})|\,\phi_{L'}(\mathbf{k})\rangle = \delta_{LL'}$. The effective density of states for the L-channel is written as:

$$N_L(0)\sim\int\frac{\mathrm{d}l_{\mathbf{k}}}{v_F(\mathbf{k})}\left|\phi^2_L(\mathbf{k})\right|.$$

Equations (7) and (8) state that in elementary superconductors $\lambda_{L,\nu}(\mathbf{k})$ does not depend on the atomic mass since the matrix element is proportional to the ion displacement, that is $g_\nu(\mathbf{k},\mathbf{k}')\sim 1/\sqrt{M\Omega}$ and the resulting $\lambda_\nu\sim 1/M\Omega^2\sim 1/\kappa$ is then independent of M. However, since in structurally complicated high$-T_\mathrm{c}$ cuprates $\lambda_{L,\nu}(\mathbf{k})$ depend on the components of the phonon eigenvectors, they can be influenced by the site-selective substitution. We investigate the electron-phonon coupling in two

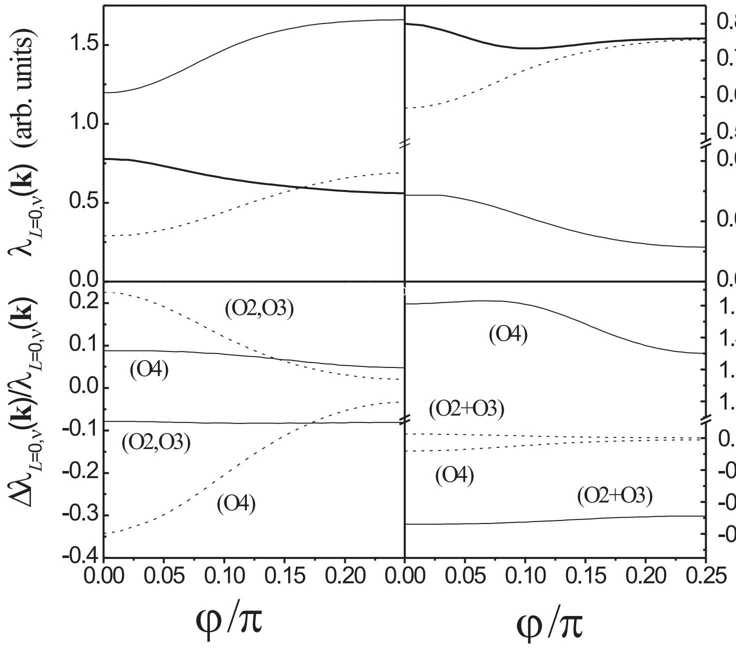

Fig. 4. $\lambda_{L=0,\nu}(\mathbf{k})$ for the modes which give considerable contributions to the electrons-phonon coupling (upper panel). The $\mathbf{k}$-dependences of the changes arising due to the site-selective substitution $\Delta\lambda_{L=0,\nu}(\mathbf{k})/\lambda_{L=0,\nu}(\mathbf{k})$ (lower panel). The notations and indications are the same as in Figure 2. Left and right panel corresponds to $\hat{H}^{(\mathrm{ap})}_{\mathrm{e-p}}$ and $\hat{H}^{(\mathrm{pl})}_{\mathrm{e-p}}$, respectively. The angle φ is introduced in Figure 3.

symmetry channels: $L=0$ (s-channel, $\phi_0(\mathbf{k}) \sim$ const.) and $L=2$ (d-channel, $\phi_2(\mathbf{k}) \sim \cos(2\varphi)$) which contribute to the s- and the $d_{x^2-y^2}$-wave pairing, respectively. In this case each $\lambda_{L,\nu}(\mathbf{k})$ is modified by the site-selective substitution but the sum over all phonon modes remains constant. These changes are shown in Figure 4 for the s-channel and in Figure 5 for the d-channel. Changes in $\lambda_{L,\nu}(\mathbf{k})$ which keep λ_L constant can cause a shift in the transition temperature due to the strong-coupling effects [31]. However, the shift is relatively small.

For the phonons which are not close in frequency to the others, the changes in $\lambda_{L,\nu}(\mathbf{k})$ can be investigated within perturbation theory with $\delta\hat{D}(\mathbf{q}) = \tilde{\hat{D}}(\mathbf{q}) - \hat{D}(\mathbf{q})$ being considered as a perturbation. The changes in the eigenvectors are given, therefore, by:

$$\delta\mathbf{U}_\nu(\mathbf{q}) = \sum_{\nu'\neq\nu} \frac{\langle \mathbf{U}_{\nu'}(\mathbf{q})|\,\delta\hat{D}(\mathbf{q})\,|\mathbf{U}_\nu(\mathbf{q})\rangle}{\Omega_\nu^2(\mathbf{q}) - \Omega_{\nu'}^2(\mathbf{q})}\mathbf{U}_{\nu'}(\mathbf{q}). \qquad (9)$$

For the full substitution $\delta\hat{D}(\mathbf{q}) = (\eta^2-1)\hat{D}(\mathbf{q})$, therefore, no changes in the eigenvector arise since $\langle \mathbf{U}_{\nu'}(\mathbf{q})|\,\hat{D}(\mathbf{q})\,|\mathbf{U}_\nu(\mathbf{q})\rangle = \Omega_\nu^2(\mathbf{q})\delta_{\nu\nu'}$. In the case of site-selective substitutions $\delta\mathbf{U}_\nu(\mathbf{q})$ is finite. An estimate of $|\delta\mathbf{U}_\nu(\mathbf{q})| \sim (1-\eta)\max\left[D_{\xi\xi'}(\mathbf{q})/\left(\Omega_\xi^2(\mathbf{q}) - \Omega_{\xi'}^2(\mathbf{q})\right)\right]$, where the indices ξ, ξ' correspond to the interaction between the apical and the plane oxygen ions, shows that the changes in the eigenvectors has the same order of magnitude as the changes in the frequencies. Since the electron-phonon coupling is directly related to the components of the eigenvectors, the relative changes in $\lambda_{L,\nu}$ are of the

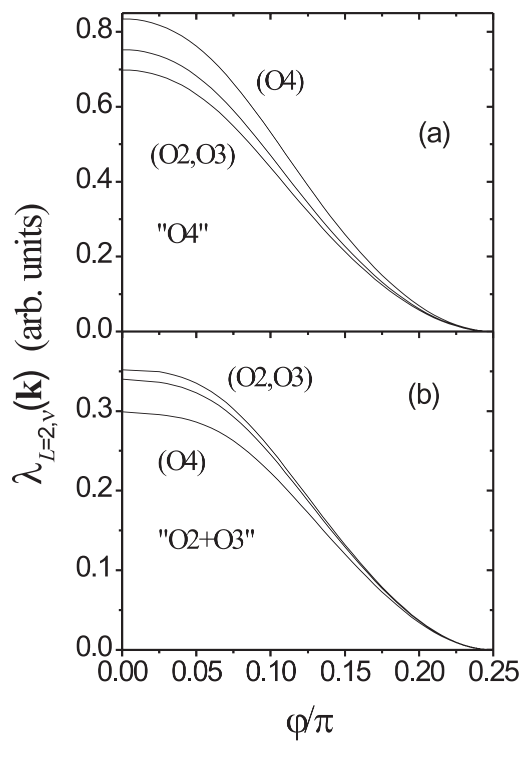

Fig. 5. The $\mathbf{k}$-dependences of $\lambda_{L=2,\nu}(\mathbf{k})$ for two phonon modes (indicated in the figures) for different types of substitution. (a) $\hat{H}^{(\mathrm{ap})}_{\mathrm{e-p}}$ coupling, (b) $\hat{H}^{(\mathrm{pl})}_{\mathrm{e-p}}$ coupling. The type of the substitution is indicated near the lines. Lines without indication correspond to non-substituted crystals. The angle φ is introduced in Figure 3.

same order of magnitude. This estimate is not sensitive to the details of electronic structure, lattice dynamics, and electron-phonon coupling. However, for O4 and O2+O3 modes being close in frequency the perturbative approach is not valid.

A possible influence of the site-selective substitution on the the carrier effective mass should be mentioned here. The effect of the full substitution appeared to be rather strong, *i.e.* of the order of few percent [32]. The isotope influence on the carrier mass can be regarded as a polaronic effect, since the effective mass of the itinerant carrier $m^* = m(1+\lambda)$ remains constant after the complete substitution. (Here m is the effective mass due to the periodic lattice potential.) Within our model, which neglects polaronic effects, the effective mass is not sensitive to the site-selective isotope substitution either. For polarons, the dependence of the effective mass on the coupling constant and the phonon frequency is more complicated [33], leading to the isotope effect on the effective mass. Experimental observation of these site-selective substitutions on the effective mass will shed light on the origin of the carriers in the HTSC and their coupling to the lattice.

To conclude, we have considered the influence of the site-selective isotope substitution in high-T_{c} cuprates on (i) electron-phonon coupling for Raman active phonons and (ii) $\lambda_{L,\nu}(\mathbf{k})$ in two symmetry channels ($L = 0$ and $L = 2$). Contrary to the full substitution, which does not change $\lambda_{L,\nu}(\mathbf{k})$, site-selective substitution can increase or decrease it. The effect which arises due to the changes in the eigenvectors of the vibrations for some modes can be much stronger than the changes in their frequencies.

This work was supported by the Austrian Science Fund *via* the project M591-TPH. We are grateful to P.B. Allen for valuable remarks and to H. Auer for fruitful collaboration.

References

1. A comprehensive review of conventional superconductors can be found in: P.B. Allen, B. Mitrovic in *Solid Sate Physics* **37**, edited by H. Ehrenreich, F. Seitz, D. Turnbull (Academic Press, NY, 1982).
2. For a review see A.V. Chubukov, D. Pines, J. Schmalian, to appear in *The Physics of Conventional and Unconventional Superconductors* edited by K.H. Bennemann, J.B. Ketterson (Springer-Verlag), preprint `cond-mat/0201140`.
3. O.K. Andersen, A.I. Liechtenstein, O. Rodriguez, I.I. Mazin, O. Jepsen, V.P. Antropov, O. Gunnarsson, S. Gopalan, Physica C **185-189**, 147 (1991).
4. O.K. Andersen, A.I. Liechtenstein, O. Jepsen, F. Paulsen, J. Phys. Chem. Solids **56**, 1573 (1995).
5. O. Jepsen, O.K. Andersen, I. Dasgupta, S.Y. Savrasov, J. Phys. Chem. Solids **59**, 1718 (1998).
6. S.Y. Savrasov, O.K. Andersen, Phys. Rev. Lett. **77**, 4430 (1996).
7. Z.-X. Shen, A. Lanzara, N. Nagaosa, preprint `cond-mat/0102244` (unpublished).
8. B. Batlogg, G. Kourouklis, W. Weber, R.J. Cava, A. Jayaraman, A.E. White, K.T. Short, L.W. Rupp, E.A. Rietman, Phys. Rev. Lett. **59**, 912 (1987), T.A. Faltens, W.K. Ham, S.W. Keller, K.J. Leary, J.N. Michaels, A.M. Stacy, H. zur Loye, D.E. Morris, T.W. Barbee III, L.C. Bourne, M.L. Cohen, S. Hoen, A. Zettl, *ibid.*, p. 915.
9. J. Labbe, J. Bok, Europhys. Lett. **3**, 1225 (1987).
10. R. Combescot, J. Labbe, Phys. Rev. B **38**, 262 (1988), C.C. Tsuei, D.M. Newns, C.C. Chi, P.C. Pattnaik, Phys. Rev. Lett. **65**, 2724 (1990), A.A. Abrikosov, J.C. Campuzano, K. Gofron, Physica C **214**, 73 (1993).
11. R. Zeyher, Z. für Physik B **97**, 3 (1995).
12. M. Cardona, R. Liu, C. Thomsen, W. Kress, E. Schönherr, M. Bauer, L. Genzel, W. König, Solid State Commun. **67**, 789 (1988).
13. D. Zech, H. Keller, K. Conder, E. Kaldis, E. Liarokapis, N. Poulakis, K.A. Müller, Nature **371**, 681 (1994).
14. J.H. Nickel, D.E. Morris, J.W. Ager, Phys. Rev. Lett. **70**, 81 (1993).
15. V.B. Vykhodets, T.E. Kurennykh, V.A. Pavlov, A.A. Fotiev, JETP Lett. **58**, 431 (1993).
16. S.I. Bredikhin, A.A. Maksimov, B.C.H. Steele, I.I. Tartakovskii, Physica C **196**, 112 (1992).
17. Recent review on different experimental manifestations of the isotope effects in HTSC can be found in G.-M. Zhao, H. Keller, K. Conder, J. Phys. Cond. Matt. **13**, R569 (2001).
18. C. Ambrosch-Draxl, H. Auer, R. Kouba, E.Ya. Sherman, P. Knoll, M. Mayer, Phys. Rev. B **65**, 064501 (2002).
19. M. Opel, R. Hackl, T.P. Devereaux, A. Virosztek, A. Zawadowski, A. Erb, E. Walker, H. Berger, L. Forro, Phys. Rev. B **60**, 9836 (1999).
20. O.K. Andersen, S.Y. Savrasov, O. Jepsen, A.I. Liechtenstein, J. Low Temp. Phys. **105**, 285 (1996).
21. K. Gofron, J.C. Campuzano, A.A. Abrikosov, M. Lindroos, A. Bansil, H. Ding, D. Koelling, B. Dabrowski, Phys. Rev. Lett. **73**, 3302 (1994), E.Ya. Sherman, O.V. Misochko, Phys. Rev. B **59**, 195 (1999).
22. E.I. Rashba, E.Ya. Sherman, JETP Lett. **47**, 482 (1988).
23. T.P. Devereaux, A. Virosztek, A. Zawadowski, Phys. Rev. B **51**, 501 (1995).
24. E. Pavarini, I. Dasgupta, T. Saha-Dasgupta, O. Jepsen, O.K. Andersen, Phys. Rev. Lett. **87**, 047003 (2001).
25. O.V. Misochko, E.Ya. Sherman, N. Umesaki, K. Sakai, S. Nakashima, Phys. Rev. B **59**, 11 495 (1999).
26. V.G. Hadjiev, X. Zhou, T. Strohm, M. Cardona, Q.M. Lin, C.W. Chu, Phys. Rev. B **58**, 1043 (1998).
27. E.Ya. Sherman, O.V. Misochko, Phys. Rev. B **63**, 104520 (2001).
28. The role of isotope disorder on optical spectra of molecular crystals was considered in V.L. Broude. E.I. Rashba, E.F. Sheka, *Spectroscopy of molecular excitons*, Springer Series in Chemical Physics **16** (Springer, 1985), p. 271. The mechanism of the site-selective isotope effect on Raman scattering [18] is qualitatively different to the mechanisms proposed for the absorption spectra of molecular solids.
29. G.M. Eliashberg, Sov. Phys. JETP **11**, 696 (1960), Sov. Phys. - JETP **12**, 1000 (1961).
30. W.L. McMillan, Phys. Rev. **167**, 331 (1968).
31. We are grateful to P.B. Allen, who brought this fact to our attention.
32. G.-M. Zhao, D.E. Morris, Phys. Rev. B **51**, R16487 (1995), G.-M. Zhao, M.B. Hunt, H. Keller, K.A. Müller, Nature **385**, 236 (1997), G.-M. Zhao, V. Kirtikar, D.E. Morris, Phys. Rev. B **63**, R220506 (2001).
33. A.S. Alexandrov, N.F. Mott, Int. J. Mod. Phys. **8**, 2075 (1994), D. Mihailovic, V. Kabanov, Rev. B **63**, 054505 (2001).